First principles study of the ferromagnetism in $Ga_{1-x}Mn_xAs$ semiconductors

2004 J. Phys.: Condens. Matter 16 8243

(http://iopscience.iop.org/0953-8984/16/46/011)

INSTITUTE OF PHYSICS PUBLISHING JOURNAL OF PHYSICS: CONDENSED MATTER

J. Phys.: Condens. Matter **16** (2004) 8243–8250 PII: S0953-8984(04)85132-4

First principles study of the ferromagnetism in $Ga_{1-x}Mn_xAs$ semiconductors

Antônio J R da Silva[1], A Fazzio[1], Raimundo R dos Santos[2] and Luiz E Oliveira[3]

[1] Instituto de Física, Universidade de São Paulo, CP 66318, 05315-970, São Paulo, SP, Brazil
[2] Instituto de Física, Universidade Federal do Rio de Janeiro, CP 68528, 21945-970 Rio de Janeiro, RJ, Brazil
[3] Instituto de Física, Unicamp, CP 6165, 13083-970 Campinas, SP, Brazil

Received 16 August 2004, in final form 11 October 2004
Published 5 November 2004
Online at stacks.iop.org/JPhysCM/16/8243
doi:10.1088/0953-8984/16/46/011

Abstract

We have performed *ab initio* calculations within the density-functional theory for $Ga_{1-x}Mn_xAs$ diluted semiconductors. Total energy results unambiguously show that a quasi-localized $\downarrow$ hole, with predominant p-like character, surrounds the fully polarized Mn $\uparrow$ d^5-electrons. The calculations indicate that the holes form a relatively dispersionless impurity band, thus rendering effective-mass descriptions of hole states open to challenge. We obtain estimates both for the $s = 1/2$ hole and $S = 5/2$ Mn exchange coupling, and for the distance dependence of the effective Mn–Mn exchange interaction. The results demonstrate that the effective Mn–Mn coupling is always ferromagnetic, and thus non-RKKY, and is intermediated by the antiferromagnetic coupling of each Mn spin to the holes.

(Some figures in this article are in colour only in the electronic version)

In the last few years, a considerable amount of work has been devoted to the study of diluted magnetic semiconductors (DMS), since the possibility of manipulating both the charge and spin degrees of freedom of carriers in magnetic materials will change qualitatively the efficiency of spintronics devices. The discovery of hole-induced ferromagnetism in p-type (In, Mn)As systems [1] was followed by the successful growth of ferromagnetic (Ga, Mn)As alloys [2]. A quantitative understanding of the physics in these materials is therefore crucial, since ferromagnetic III–V alloys may be readily combined into semiconductor heterostructure systems, opening up a range of applications of optoelectronic devices through the combination of quantum and magnetic phenomena in these materials. However, in order to develop full-scale applications, one needs to elucidate several issues in relation to these systems. In the case of $Ga_{1-x}Mn_xAs$ semiconductors, it is well known that Mn forms acceptors when in substitutional Ga lattice sites (Mn_{Ga}). One of the standing issues is related to the fact

that the critical temperature and hole concentration, as a function of Mn composition in $Ga_{1-x}Mn_xAs$, are crucially dependent on the details of the growth conditions [3–14], even in as-grown samples; note, in particular, that for $x \simeq 5\%$, T_c ranges from ∼30 to 110 K, with the highest temperature [4] of 110 K only being reproduced by other groups after post-growth annealing [6, 12, 15]. The measured hole concentration p as a function of x similarly reveals discrepancies both in trends and in order of magnitude; note that different experimental techniques (Hall resistance [6] and Raman scattering [8]) applied to the same $x = 0.083$ sample yield values of p differing by as much as a factor of 10.

From the theoretical point of view, different models have been proposed to describe the electronic and magnetic properties of (Ga, Mn)As. The generally accepted view is that a given Mn ion interacts with the holes via a local antiferromagnetic Kondo-like exchange coupling between their magnetic moments [5, 16, 17]; this interaction is thought to lead to a polarization of the hole subsystem, which would then give rise to an effective ferromagnetic coupling between the Mn moments. Early attempts treated the holes within an sp parabolic-band effective-mass approximation; this approach is in conflict with recent photoemission studies [9, 18] and infrared measurements [19], which indicate that the holes form a relatively flat impurity band at the Fermi energy, instead of residing in an unaltered GaAs valence band. In particular, infrared spectroscopic measurements estimated the hole effective mass within the range $0.7m_e < m^* < 15m_e$ for an $x = 0.52$ sample, and even larger values at higher dopings [19]. As a consequence, any treatment of holes within an effective-mass approximation, including attempts in the direction of incorporating aspects such as a Kohn–Luttinger treatment of the valence states [20, 21], are quite clearly open to question. The same applies to experimental estimates of the $S = 5/2$ Mn ion–hole exchange coupling which resort to effective-mass models to fit resistivity data [4, 17, 22]. Another point which is a matter of debate concerns the nature of the effective Mn–Mn interaction: distinct electronic structure calculations together with a Heisenberg spin Hamiltonian do not agree whether the effective coupling becomes antiferromagnetic for some distance or not [23, 24].

In order to settle these issues, we have performed a detailed *ab initio* study of the origin of the Mn–Mn ferromagnetic coupling in $Ga_{1-x}Mn_xAs$ DMS [25]. Our total energy calculations are based on the density-functional theory (DFT) within the generalized-gradient approximation (GGA) for the exchange–correlation potential, with the electron–ion interactions described using ultrasoft pseudopotentials [26]. A plane wave expansion up to 230 eV as implemented in the VASP code [27] was used, together with a 128-atom and a 250-atom fcc supercell and the L-points for the Brillouin zone sampling. The positions of all atoms in the supercell were relaxed until all the force components were smaller than 0.02 eV $Å^{-1}$. We have also checked for spin–orbit effects through the projector augmented-wave (PAW) method [28] and found that they may be safely neglected[4].

Let us first consider the case of a single isolated Mn_{Ga} acceptor, in which case we have performed total energy calculations for a 250-atom supercell, and for neutral $(Mn_{Ga})^0$ and negatively charged $(Mn_{Ga})^-$ defects. In figure 1, we compare the density of states (DOS) for each spin channel, in the cases of pure GaAs and with one Mn atom. We see that for the up-spin channel the main effect of this impurity is to add spectral weight at the Fermi level (for completeness, it should be mentioned that the defect also adds spectral weight to the bottom of the conduction band, in the case of the down-spin channel), with a width of the order of 0.3 eV.

[4] In the case of two nearest-neighbour Mn defects in a 128-atom supercell, we have considered spin–orbit effects within the PAW method (cf [28]) as implemented in the VASP code, and found a change from 0.29 to 0.24 eV in the total energy difference between the excited antiferromagnetic and ground state ferromagnetic Mn-spin alignments. As this change is not substantial, we therefore choose to ignore spin–orbit effects in the total energy calculations presented in this work.

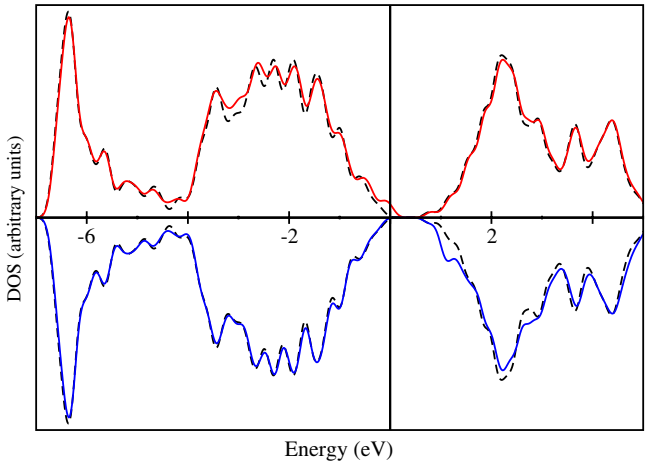

Figure 1. Density of states (arbitrary units) for the Mn_{Ga} defect (solid curves) and for the pure GaAs crystal (broken curves). Curves on the top (bottom) panel are for spin up (down). The vertical line at 0 eV marks the Fermi energy.

As discussed by Sanvito *et al* [22], this peak does not scale with Mn concentration, indicating that these states form an impurity band. We have also evaluated the binding energy of the acceptor state as 0.1 eV, which is in quite good agreement with the experimental value of 0.11 eV for the single Mn acceptor level [29, 30].

Moreover, the ground state of the Mn_{Ga} defect is consistent with the picture of a $\downarrow$ hole interacting antiferromagnetically with the $\uparrow$ $S = 5/2$ spin of the d^5-configuration at the Mn site. The robustness of this state is illustrated by the fact that the ferromagnetic (high-spin) configuration with a $\uparrow$ hole lies $\simeq$0.25 eV above the antiferromagnetic (low-spin) one. Figures 2(a) and (c) show the difference $m(\mathbf{r}) \equiv \rho_\uparrow(\mathbf{r}) - \rho_\downarrow(\mathbf{r})$ for the Mn_{Ga} defect, where ρ_σ is the total charge density in the σ-polarized channel. We note that, near the Mn_{Ga} acceptor, the local magnetization has a strong $\uparrow$ d-like character, due essentially to the valence-band resonant d^5 electrons, whereas as one approaches its As neighbours, the character changes to $\downarrow$ p-like. The signature of the above-mentioned antiferromagnetic interaction consists of a sign change in $m(\mathbf{r})$ as one moves from the Mn site to any of its As neighbours. For Mn, we obtain a magnetic moment of 4.1 μ_B, whereas for its four As first-nearest neighbours we obtain -0.03 μ_B, similarly to what has been reported in the literature [22]. In order to probe the extent of the perturbation in the charge density associated with the Mn_{Ga} defect, the difference between $\rho_\uparrow(\mathbf{r}) + \rho_\downarrow(\mathbf{r})$ calculated for the Mn_{Ga} state and the GaAs host is depicted in figures 2(b) and (d). One clearly notes that the excess charge is essentially confined within the region surrounding the Mn site, which indicates the localized nature of the holes. This is also evident from the corresponding contour plots, presented in figures 2(c) and (d), respectively. For all values of the magnetization and of the excess charge, the contour plots are restricted to the region very near the defect—around 8 Å; this should be contrasted with the case of shallow defects, whose contour plots lead to states spreading through the whole cell. This, together with the appearance of a rather narrow peak near the Fermi energy, can be taken as evidence in favour of localized impurity states.

The origin of ferromagnetism in diluted $Ga_{1-x}Mn_xAs$ semiconductors may be elucidated by focusing on interacting Mn_{Ga} substitutional defects in a 128-atom supercell, considering both a ferromagnetic as well as an antiferromagnetic alignment between the Mn spins.

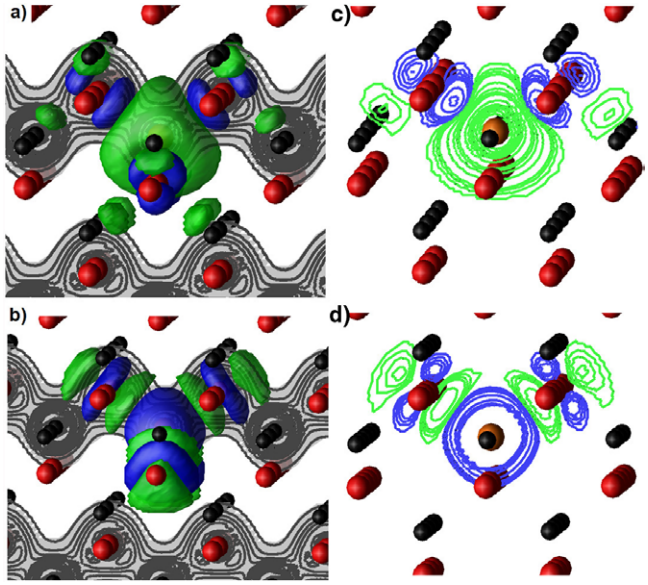

Figure 2. Isosurfaces for (a) the net local magnetization $m(\mathbf{r}) = \rho_\uparrow(\mathbf{r}) - \rho_\downarrow(\mathbf{r})$ for the Mn_{Ga} defect, and (b) the difference between $\rho_\uparrow(\mathbf{r}) + \rho_\downarrow(\mathbf{r})$ calculated for the Mn_{Ga} ground state and the GaAs host. The lighter (green, in the online version) surface corresponds to a value of $+0.004e$ Å^{-3}, and the darker (blue online) surface to $-0.004e$ Å^{-3}; for comparison, note that a uniform charge density of 1 electron/unit cell in GaAs corresponds to $+0.022e$ Å^{-3}, with e being the electron charge. The darker (black online) and lighter (red online) spheres denote the Ga and As atoms. Contour plots (in e Å^{-3}) for the local magnetizations of (a) and (b) are shown in (c) and (d), respectively. The lighter (green online) lines represent positive values, and the darker (blue online) ones negative values; their values are -0.3, -0.2, -0.1, -0.008, -0.006, -0.004, -0.002, 0.002, 0.004, 0.006, 0.008, 0.02, 0.04, 0.06, 0.08, 0.2, 0.4, 0.6, 0.8, 1.0, 1.5 and 2.0 in (c) and -0.1, -0.08, -0.06, -0.04, -0.02, -0.01, -0.008, -0.006, -0.004, 0.004, 0.006, 0.008, 0.01 and 0.02 in (d).

We have performed calculations for two Mn substitutional atoms (two Mn in a 128-atom supercell corresponds to a Mn concentration $x \simeq 0.031$) in configurations corresponding to all inequivalent positions within the supercell, i.e., Mn–Mn distances varying from 4.06 Å up to 11.48 Å. Our total energy results yield an unambiguous Mn–Mn ferromagnetic ground state in all cases (see footnote 4). Figures 3(a)–(d) show the net magnetization $m(\mathbf{r})$ isosurfaces for two Mn defects in nearest-neighbour and next-nearest-neighbour positions (for the Ga sublattice), with parallel and antiparallel Mn spins. In figure 3, the Mn atoms are at the centre of the spherical-like regions of $m(\mathbf{r})$, whereas the p-like regions are always centred on As atoms. Note that, irrespective of the relative orientation of the Mn–Mn spins, the antiferromagnetic coupling between the Mn and hole spins is always maintained. In the Mn–Mn antiferromagnetic case, this leads to the appearance of nodes in $m(\mathbf{r})$, which contribute to increase its energy relative to the ferromagnetic state.

Each panel ((e)–(h)) on the right-hand side of figure 3 shows the contour plots corresponding to the isosurfaces on the left. The overall features confirm, again, that the Mn–Mn defect is essentially localized, although the magnetization density clearly spreads out from one Mn_{Ga} site to the other. The picture that emerges is that of a cloud of $\downarrow$ holes surrounding the substitutional Mn, with the distribution of quasi-localized holes, of predominant p-like character, giving rise to a relatively flat impurity band, so that a description via the effective-mass approximation would be inappropriate; this is in agreement with angle-

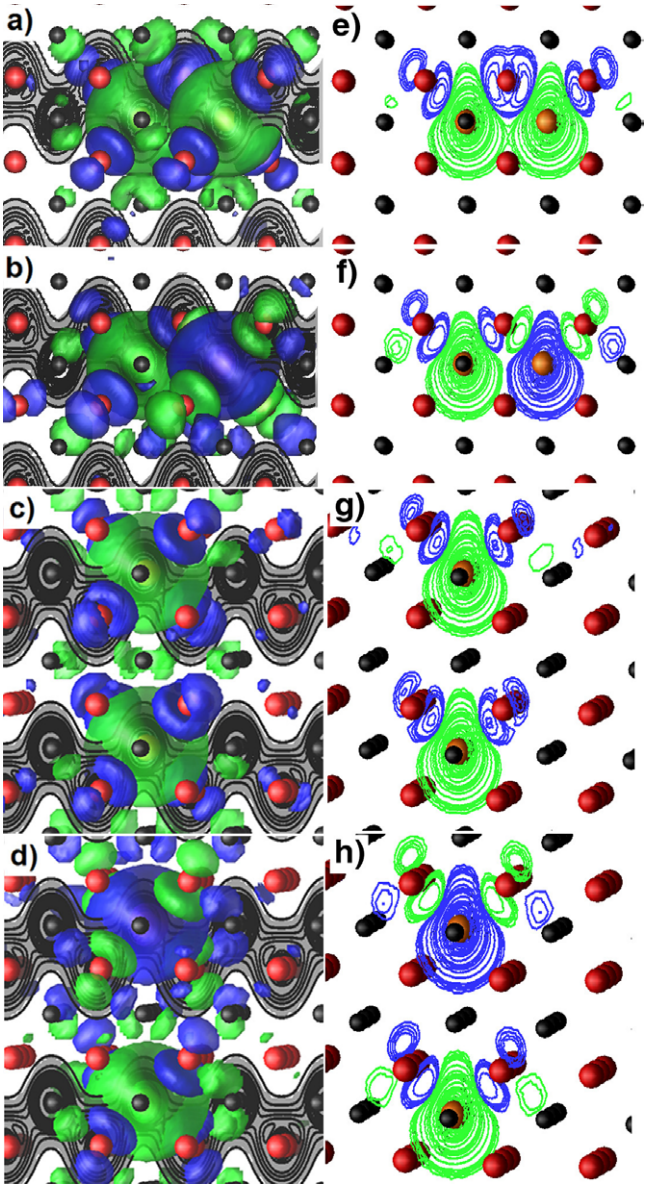

Figure 3. Isosurfaces for the net local magnetization $m(\mathbf{r}) = \rho_\uparrow(\mathbf{r}) - \rho_\downarrow(\mathbf{r})$ in the case of two Mn_{Ga} defects; the greyscale (colour online) code and isosurface values are the same as in figure 2. In (a) and (b) ((c) and (d)) the two Mn are nearest neighbours (next-nearest neighbours) with their $S = 5/2$ spins aligned parallel and antiparallel, respectively. Contour plots (in e Å^{-3}) for the local magnetizations of (a) and (b) ((c) and (d)) are shown in (e) and (f) ((g) and (h)), respectively. The lighter (green online) lines represent positive values, and the darker (blue online) ones negative values; their values are -0.03, -0.02, -0.01, -0.008, -0.006, -0.004, 0.004, 0.006, 0.008, 0.01, 0.02, 0.04, 0.06, 0.08, 0.1, 0.2, 0.4, 0.6, 0.8, 1.0, 1.5 and 2.0 in (e) and (g) and ± 0.004, ± 0.006, ± 0.008, ± 0.01, ± 0.02, ± 0.04, ± 0.06, ± 0.08, ± 0.1, ± 0.2, ± 0.4, ± 0.6, ± 0.8, ± 1.0, ± 1.5 and ± 2.0 in (f) and (h).

resolved photoemission measurements [18], which suggest an almost non-dispersive Mn-induced impurity band of width $\lesssim$0.5 eV.

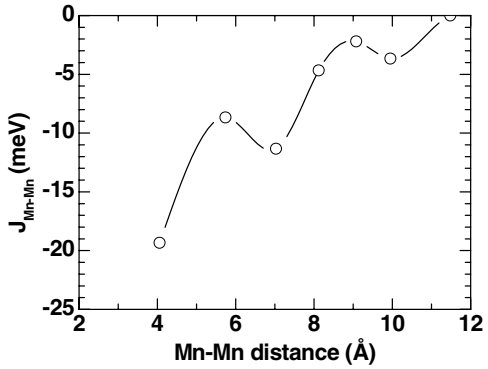

Figure 4. Exchange coupling $J_{\mathrm{Mn-Mn}}$ between Mn atoms in $Ga_{1-x}Mn_xAs$ alloys, versus the Mn–Mn distance. Open dots are our calculated results whereas the full curve is a guide to the eye.

As a by-product, we have also calculated the total energy difference between high- and low-spin configurations associated with the $s = 1/2$ hole and $S = 5/2$ Mn spins. Assuming a coupling of the type $J_{\mathrm{Mn-h}}\mathbf{s}\cdot\mathbf{S}$, where $\mathbf{s}$ acts on quasi-localized holes and $\mathbf{S}$ on the localized Mn orbitals, the high- and low-spin energy levels are given by $E = \frac{1}{2}J_{\mathrm{Mn-h}}(S_{\mathrm{tot}}^2 - s^2 - S^2)$, where $S_{\mathrm{tot}} = 3$ or 2 for high- and low-spin configurations, respectively. The strength of the exchange coupling is then calculated as $J_{\mathrm{Mn-h}} = \Delta E/3 \sim +0.1$ eV. We would like to stress that the interaction $J_{\mathrm{Mn-h}}\mathbf{s}\cdot\mathbf{S}$ should be viewed as an effective one which reproduces the energy difference between high- and low-spin configurations. In this sense, the value of $J_{\mathrm{Mn-h}}$ we obtain should not be compared with the one arising from the mean-field Zener model [20], since in the latter approach the corresponding operator $\mathbf{s}$ acts on extended hole states.

We now turn to one of our main objectives, namely a scenario for the effective coupling between Mn spins. To this end, from total energy calculations we have evaluated the effective exchange coupling between pairs of $S = 5/2$ Mn spins, $J_{\mathrm{Mn-Mn}}$, as a function of the Mn–Mn distance, for all inequivalent pair positions within the supercell (for an Mn–Mn interaction modelled through $J_{\mathrm{Mn-Mn}}\mathbf{S}_{\mathrm{Mn}_i}\cdot\mathbf{S}_{\mathrm{Mn}_j}$). In figure 4 we display the theoretical predictions for $J_{\mathrm{Mn-Mn}}$. The results clearly show that the coupling between the Mn spins is always ferromagnetic, irrespective of their relative distance. As it is well known that the bare coupling between two Mn spins should be antiferromagnetic, one concludes that the resulting Mn–Mn ferromagnetic effective coupling, in $Ga_{1-x}Mn_xAs$, is essentially intermediated by the antiferromagnetic coupling of each Mn spin to the quasi-localized holes. Also, the observed non-monotonic behaviour of $J_{\mathrm{Mn-Mn}}(\mathbf{r})$ should be attributed to the anisotropic character of the effective interaction, as it may be inferred from figure 3. One should notice that the supercell sizes we use to calculate the interaction between two Mn spins in bulk GaAs are definitely more realistic than simpler approaches adopted in previous works. Nevertheless, the results of Bouzerar *et al* [23], though they have been obtained through a non-full-potential tight-binding linear muffin-tin orbital method, are in qualitative agreement with our findings. Also, recent calculations by Zhao *et al* [31], using a method similar to ours, though with smaller supercells, found similar anisotropic behaviour for the exchange coupling. Moreover, the present total energy calculations unambiguously rules out the possibility of a typical RKKY oscillation with positive and negative values of the exchange couplings, as inferred from the naive CPA approach by Sandratskii and Bruno [24], and indeed found in the case of Mn_xGe_{1-x} [32]. Moreover, figure 3 shows that $J_{\mathrm{Mn-Mn}}$ essentially decreases with Mn–Mn separation and vanishes above $\simeq$10–12 Å; this is in contrast with the conclusion of Sanyal *et al* [33] that the strength of

the ferromagnetic coupling between Mn spins is not decreased substantially for large Mn–Mn separation.

The data in figure 4 can be used to estimate the critical temperature at a given Mn concentration, which, within a simple mean-field theory is given by

$$k_B T_c = \frac{S(S+1)}{3}|J_0|, \tag{1}$$

with

$$J_0 = \sum_{\mathbf{r}} J(\mathbf{r}) = \left(\frac{\overline{z_1}}{2}J_1 + \frac{\overline{z_2}}{2}J_2 + \frac{\overline{z_3}}{2}J_3 + \cdots\right), \tag{2}$$

where $J_1, J_2, \ldots$ stand for first-, second-,. . ., -neighbour interactions, the values of which are given in figure 4, and the $\overline{z_i}$ are the corresponding configurationally averaged coordination numbers in the Ga sublattice. If we take $\overline{z_i} = xz_i$, with x being the fraction of Mn sites, one obtains $T_c \simeq 1.2 \times 10^4 x$ K, in qualitative agreement with the low-density behaviour observed experimentally [4]; we note that not every Mn atom contributes with a hole, so that the above result may be overestimated by a factor of the order of 30% [17].

One should mention that the discrepancies between different experimental data indicate that the magnetic, structural, and electronic properties of as-grown $Ga_{1-x}Mn_xAs$ alloys are extremely sensitive to the actual molecular-beam epitaxy (MBE) growth conditions, such as, for example, growth temperature and beam flux ratios. In fact, this is to be expected, since the holes provided by the Mn_{Ga} acceptors may be compensated by defects such as As antisite (As_{Ga}) donors, Mn interstitials (Mn_I), Mn_I–Mn_{Ga} pairs, MnAs complexes, etc. Of course, the situation with respect to annealed $Ga_{1-x}Mn_xAs$ samples is rather more complicated, and a proper analysis of experimental measurements performed in after-annealing samples must involve a realistic modelling of diffusion processes involving several defects, formation of random precipitates, clustering effects, etc. Therefore, we emphasize that a proper understanding of the physics of $Ga_{1-x}Mn_xAs$ alloys must involve a microscopic description of the effect of different defects on their electronic and magnetic properties.

In conclusion, we have provided a detailed *ab initio* study of the physical origin of the Mn–Mn ferromagnetic coupling, by considering isolated Mn_{Ga} defects, as well as two substitutional Mn atoms per supercell, in various relative positions. Our total energy calculations provide unambiguous evidence that the effective coupling is always ferromagnetic, and thus non-RKKY, and is intermediated by an antiferromagnetic coupling of each Mn spin to the quasi-localized holes.

Acknowledgments

Partial financial support by the Brazilian Agencies CNPq, CENAPAD-Campinas, Rede Nacional de Materiais Nanoestruturados/CNPq, FAPESP, FAPERJ, and Millenium Institute for Nanosciences/MCT is gratefully acknowledged.

References

[1] Ohno H, Munekata H, Penney T, von Molnàr S and Chang L L 1992 *Phys. Rev. Lett.* **68** 2664
[2] Ohno H, Shen A, Matsukura F, Oiwa A, Endo A, Katsumoto S and Iye Y 1996 *Appl. Phys. Lett.* **69** 363
[3] Van Esch A, Van Bockstal L, De Boeck J, Verbanck G, van Steenbergen A S, Wellmann P J, Grietens B, Bogaerts R, Herlach F and Borghs G 1997 *Phys. Rev.* B **56** 13103
[4] Matsukura F, Ohno H, Shen A and Sugawara Y 1998 *Phys. Rev.* B **57** R2037
[5] Ohno H 1999 *J. Magn. Magn. Mater.* **200** 110
[6] Potashnik S J, Ku K C, Chun S H, Berry J J, Samarth N and Schiffer P 2001 *Appl. Phys. Lett.* **79** 1495

[7] Edmonds K W, Wang K Y, Campion R P, Neumann A C, Foxon C T, Gallagher B L and Main P C 2002 *Appl. Phys. Lett.* **81** 3010
[8] Seong M J, Chun S H, Cheong H M, Samarth N and Mascarenhas A 2002 *Phys. Rev.* B **66** 033202
[9] Asklund H, Ilver L, Kanski J and Sadowski J 2002 *Phys. Rev.* B **66** 115319
[10] Yu K M, Walukiewicz W, Wojtowicz T, Kuryliszyn I, Liu X, Sasaki Y and Furdyna J K 2002 *Phys. Rev.* B **65** R201303
[11] Yu K M, Walukiewicz W, Wojtowicz T, Lim W L, Liu X, Sasaki Y, Dobrowolska M and Furdyna J K 2002 *Appl. Phys. Lett.* **81** 844
[12] Potashnik S J, Ku K C, Mahendiran R, Chun S H, Wang R F, Samarth N and Schiffer P 2002 *Phys. Rev.* B **66** 012408
[13] Moriya R and Munekata H 2003 *J. Appl. Phys.* **93** 4603
[14] dos Santos R R, Oliveira L E and d'Albuquerque e Castro J 2002 *J. Phys.: Condens. Matter* **14** 3751
dos Santos R R, Oliveira L E and d'Albuquerque e Castro J 2003 *J. Appl. Phys.* **93** 1845
[15] Hayashi T, Hashimoto Y, Katsumoto S and Iye Y 2001 *Appl. Phys. Lett.* **78** 1691
[16] Dietl T, Haury A and Merle d'Aubigné Y 1997 *Phys. Rev.* B **55** R3347
[17] Ohno H and Matsukura F 2001 *Solid State Commun.* **117** 179
[18] Okabayashi J, Kimura A, Rader O, Mizokawa T, Fujimori A, Hayashi T and Tanaka M 2001 *Phys. Rev.* B **64** 125304
[19] Singley E J, Kawakami R, Awschalom D D and Basov D N 2002 *Phys. Rev. Lett.* **89** 097203
[20] Dietl T, Ohno H and Matsukura F 2001 *Phys. Rev.* B **63** 195205
[21] Abolfath M, Jungwirth T, Brum J and MacDonald A H 2001 *Phys. Rev.* B **63** 054418
[22] Sanvito S, Ordejón P and Hill N A 2001 *Phys. Rev.* B **63** 165206
[23] Bouzerar G, Kudrnovský J, Berqvist L and Bruno P 2003 *Phys. Rev.* B **68** 081203(R)
[24] Sandratskii L M and Bruno P 2002 *Phys. Rev.* B **66** 134435
[25] Preliminary results were presented at the *22nd Int. Conf. on Defects in Semiconductors (Aarhus, Denmark, 2003);* da Silva A J R, Fazzio A, dos Santos R R and Oliveira L E 2003 *Physica* B **340–342** 874
[26] Vanderbilt D 1990 *Phys. Rev.* B **41** 7892
[27] Kresse G and Hafner J 1993 *Phys. Rev.* B **47** R558
Kresse G and Furthmüller J 1996 *Phys. Rev.* B **54** 11169
[28] Kresse G and Joubert D 1999 *Phys. Rev.* B **59** 1758
[29] Linnarsson M, Janzén E, Monemar B, Kleverman M and Thilderkvist A 1997 *Phys. Rev.* B **55** 6938
[30] Chapman R A and Hutchinson W G 1967 *Phys. Rev. Lett.* **18** 443
Schneider J, Kaufmann U, Wilkening W, Baeumler M and Kohl F 1987 *Phys. Rev. Lett.* **59** 240
[31] Zhao Y-J, Mahadevan P and Zunger A 2004 *Appl. Phys. Lett.* **84** 3753
[32] Zhao Y-J, Shishidou T and Freeman A J 2003 *Phys. Rev. Lett.* **90** 047204
[33] Sanyal B, Bengone O and Mirbt S 2003 *Phys. Rev.* B **68** 205210